Optical Fiber Technology 67 (2021) 102739

Contents lists available at ScienceDirect

Optical Fiber Technology

journal homepage: www.elsevier.com/locate/yofte

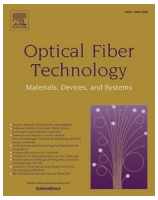

Narrow spectral linewidth and tunable erbium-doped fiber ring laser using a MZI based on CHCF

Sigifredo Marrujo-García [a], Luis A. Herrera-Piad [a,b], Iván Hernández-Romano [c,*], Daniel A. May-Arrioja [d], Vladimir P. Minkovich [e], Miguel Torres-Cisneros [a]

[a] Electronics Department, DICIS, Universidad de Guanajuato, Carretera Salamanca-Valle de Santiago km 3.5 + 1.8, Salamanca 36885, Mexico
[b] Tecnologico de Monterrey, School of Engineering and Sciences, campus Irapuato, Paseo Mirador del Valle 445, Villas de Irapuato, Irapuato, Guanajuato 36670, Mexico
[c] CONACYT-Electronics Department, DICIS, Universidad de Guanajuato, Carretera Salamanca-Valle de Santiago km 3.5 + 1.8, Salamanca 36885, Mexico
[d] Fiber and Integrated Optics Laboratory (FIOLab), Centro de Investigaciones en Óptica A.C., Aguascalientes 20200, Mexico
[e] Centro de Investigaciones en Óptica A.C., Calle Lomas del Bosque 115, León 37150, Mexico

ARTICLE INFO

Keywords:
Capillary hollow-core fiber
Tunable erbium-doped fiber ring laser
Mach-Zehnder interferometer

ABSTRACT

In this paper, a narrow spectral linewidth and wavelength-tunable erbium-doped fiber laser based on a Mach-Zehnder interferometer (MZI) as a filter is proposed and experimentally demonstrated. The filter is fabricated by splicing a short length of capillary hollow-core fiber (CHCF) between two small sections of multimode fibers (MMF). The interference pattern generated by the filter has a free spectral range of 10.5 nm and a maximum extinction ratio of 36 dB at 1560 nm. Then, by incorporating the filter inside a ring cavity laser, a single laser emission centered at 1566.46 nm with a spectral width around 0.03 nm and a high SNR of 66 dB (also has a SMSR of 53 dB) is obtained. By changing the temperature of the filter, the wavelength emission of the laser can be tuned from 1566.46 to 1570.09 nm. Considering that the fabrication process of the filter is relatively simple and can be easily implemented in an EDFL, we strongly believe that it can have a great deal of interest in telecom applications.

1. Introduction

For several years, significant effort has been devoted to the study of tunable Erbium-doped fiber lasers (TEDFLs) since they can be used in diverse applications such as telecommunication systems [1], spectroscopy [2], and optical coherence tomography [3]. The TEDFLs that are more appealing for these applications have a tunable wavelength range, a narrow linewidth, good power stability, high side-mode suppression ratio (SMSR), or signal–noise ratio (SNR). Most of these TEDFLs have been constructed by introducing a tunable fiber filter inside a cavity fiber laser. It is well-known that these filters are responsible for the attractive features of the lasers. For that reason, several fiber optic devices that work like a filter have been proposed for tuning EDFL, such as fiber Bragg gratings [4,5], Mach–Zehnder (MZI) [6–8] and Sagnac [9,10] interferometers, and nonlinear components [11]. Tunable filters also include specialty fibers like photonic crystal [12], twin-core [6], and polarization-maintaining fibers [9]. Optimizing the performance of the filters is critical since this is the key component that ultimately determines the characteristics of the laser output. For instance, J. A. Martin-Vela *et al.* [13] fabricated a MZI based on a core-offset technique covered with a thin film of aluminum to increase the contrast of the output signal (interference pattern). Using this optimized filter, they implemented a TEDFL that exhibited a better SNR (55 dB) and a tunable range from 1557 to 1560 nm. Additionally, more complex filters have been used to implement TEDFLs. For instance, Q. Zhao *et al.* [14] used a cascaded structure of two-segment Sagnac and Lyot filters to improve the laser output, obtaining a SMSR of 47 dB and a tuning range from 1530 to 1560 nm. On the other hand, TEDFLs based on specialty fibers have also been proposed; for example, Z. Tang *et al.* [15] implemented a mode interferometer using a four-leaf clover suspended core fiber. By placing this filter inside an EDFL, they demonstrated that the optical output signal showed an SNR of 55 dB and a tunable range from 1581.5 to 1546.6 nm in single-wavelength operation. Despite the good performance of these TEDFLs, it is evident that the complexity of the fabrication process increases either because of using additional fiber processing steps or when two optical devices are needed to implement an optimum laser filter. In the case of specialty fibers, the main drawback is related to the cost of the optical fiber itself.

* Corresponding author.
E-mail address: hromano@ugto.mx (I. Hernández-Romano).

https://doi.org/10.1016/j.yofte.2021.102739
Received 24 June 2021; Received in revised form 28 September 2021; Accepted 21 October 2021
Available online 31 October 2021

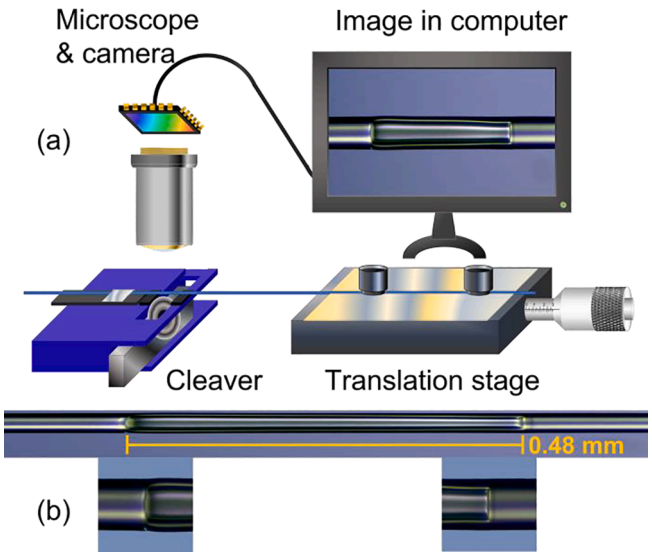

Fig. 1. (a) Experimental setup for cutting accurate lengths of optical fiber. (b) Lateral view of the MZI and the splicing section between MMF and CHCF.

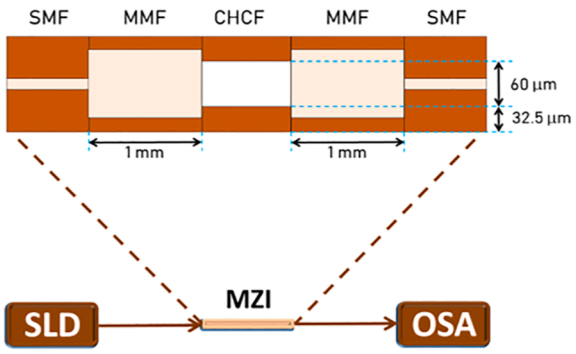

Fig. 2. Experimental setup for measuring the MZI spectral response.

In recent years, several optical fiber devices have been proposed based on capillary hollow-core fibers (CHCFs) such as FPI [16] and anti-resonant reflecting optical waveguides (ARROW) [17]. The devices based on CHCFs are attractive due to their low cost, the simple fabrication methods required to implement fiber optic devices, and because they exhibit good performance. Here, we propose a TEDFL based on a MZI that is constructed by just splicing a short length of CHCF between two sections of multimode fibers (MMF). Although the fiber filter structure is quite simple, it allows us to achieve a very narrow laser emission with a high extinction ratio. The optimum laser output shows single-wavelength emission with a linewidth around 0.03 nm, a SMSR of 53 dB, and an SNR of 66 dB. The laser emission can also be thermally tuned from 1566.46 to 1570.09 nm when the MZI is heated from 30 to 140 °C. We believe that this laser can be used for different applications since it shows minimal power and wavelength variations while exhibiting a good SNR.

2. Fabrication of the tunable fiber filter

The fabrication process of this MZI (filter) requires cutting precise fiber segments. For that season, we implemented an experimental setup with the objective of cleaving fiber segments as accurately as possible. The system contains a translation stage with a micrometer screw where the SMF is fixed in a v-groove with two magnets; the rest of the optical fiber rests on the fiber cleaver, see Fig. 1 (a). After cleaving the SMF, it is spliced either with an MMF or a CHCF. To establish the zero position of the cutting systems, the fiber is put back into the cleaver where the splicing section is above the blade. Then, the translation stage moves to a specific length with the help of the micrometer screw, and finally, an accurate segment of fiber (MMF or CHCF) is cut with the cleaver. It should be mentioned that the complete process is carried out without removing the magnets that fixed the SMF to the translation stage. Moreover, the entire process is carefully tracked with a microscope connected to a computer to control the cutting process better.

The interferometers were constructed using a CHCF whose inner and outer diameters are 65.5 and 125 µm, respectively, and an MMF (105/125 µm). The MZIs were constructed by splicing different CHCF lengths (0.3, 0.4, 0.5, 0.6, and 0.7 mm) between two sections of MMF (length of 1 mm); after that, this structure was spliced between two conventional single-mode fibers (SMF), see the zoomed image in Fig. 2. It is important to highlight that the MMF sections work as beam splitters (mode coupler). A customized program was used to splice the MMF to the CHCF, it was developed in a commercial splicer (Fitel, model s179). The most important splicing parameters are 1st Arc start power 30, 1st Arc end power 20, 1st Arc duration 2000 ms, Z push length 15 µm, Z pull start time 250 ms, and Z pull length 10 µm. The software in the splicer does not mention any unit regarding the arc power, it just lets us choose values from 0 to 255.

The experimental setup that was used to test the tunable fiber filters is shown in Fig. 2. A superluminescent diode (SLD) was used as a broadband source (SLD-1550S-A40, Thorlabs) with an available bandwidth of 100 nm, centered at 1550 nm. The output signal of the filters, which are shown in Fig. 3 (a), were measured by an Optical Spectrum Analyzer (OSA) (MS9740A, Anritsu). It should be mentioned that three sensors were fabricated for each CHCF length, and just one was selected to be shown in Fig. 3 (a). Table 1 shows some parameters of the spectrum of each filter. We consider that the insertion loss and the signal contrast are fundamental parameters for choosing the MZI tested in the laser cavity. Then, based on the results shown in Table 1, we decided to use the filter constructed with the CHCF length of 0.5 mm since the signal contrast is the largest (31.18 dB); coincidentally, it exhibits the lowest insertion loss. It is important to highlight that the CHCF lengths in Table 1 are the design lengths. The actual physical lengths will be evaluated using experimental data.

In order to determine the number of modes that generates the interference pattern, the Fast Fourier Transform (FFT) was applied to the spectra as shown in Fig. 3 (b). In all the plots, an amplitude at zero spatial frequency is observed, indicating the presence of the fundamental mode (the mode that is traveling in the free space, hollow section of the CHCF). The other amplitude whose spatial frequency changes as the CHCF length varies is related to a specific cladding mode that travels in the ring cladding (silica) of the CHCF. The working principle of this MZI can be explained with this information. First of all, it is well-known that the refractive index (RI) and the length (L) of the silica increase as the temperature augments; this is due to the thermo-optic coefficient (TOC) (8.5 × 10–6/K) [18] and the thermal expansion coefficient (TEC) (4.1 × 10–7/°C) [19]. Therefore, when the MZI is warming up, the phase of the cladding mode is modified causing a wavelength shift of the interference pattern. It should be noted that the fundamental mode is also affected by the change of the CHCF length. This mechanism can be used for tuning the laser emission.

The equation that describes the spectra of these MZIs can be written as [20]

$$I = I_f + I_h + 2\sqrt{I_f I_h}cos\Delta\phi, \quad (1)$$

where I_f and I_h are the intensity of fundamental and cladding modes, respectively. $\Delta\phi = 2\pi L\Delta n_{eff}/\lambda$ is the phase difference between the modes, where L, λ and Δn_{eff} are the length of the MZI, the wavelength of the light, and the effective refractive index difference (ERID) between these modes, respectively. The Free spectral Range (FSR) of this interference pattern is given by $FSR = \lambda^2/y\Delta n_{eff}L$, and this can be used to

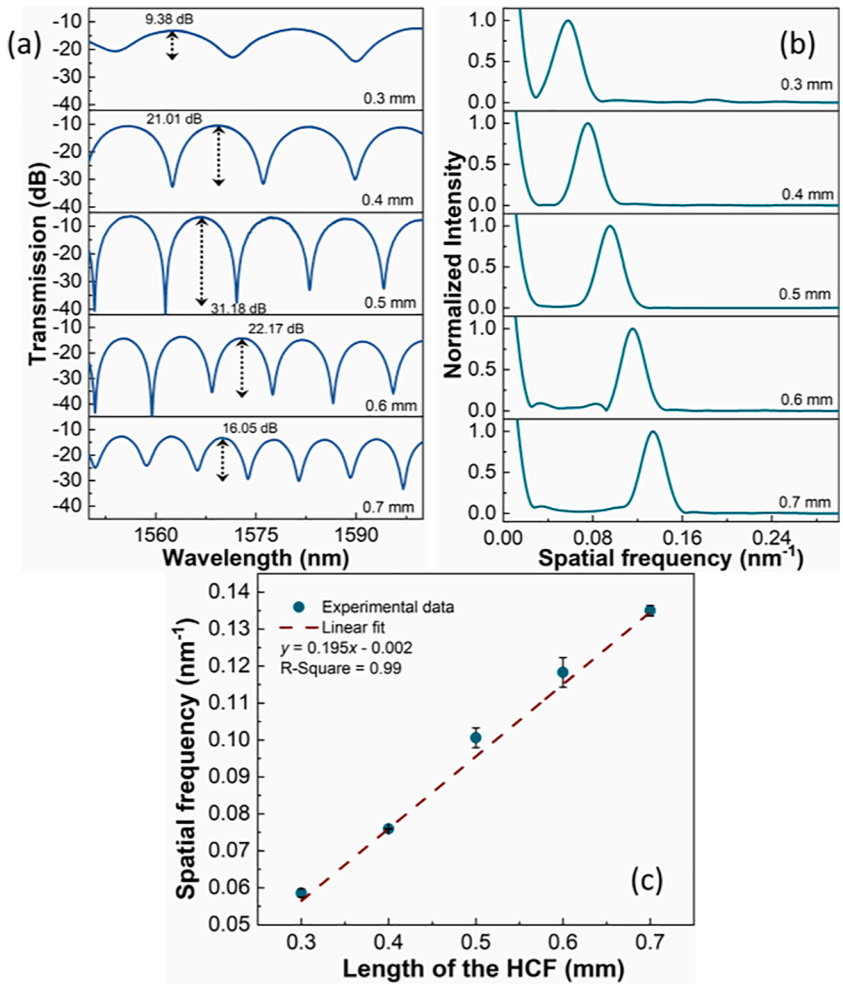

Fig. 3. Five different lengths of CHCF were used to construct MZIs. (a) Transmission spectra, (b) Spatial frequency analysis by applying the FFT to the transmission spectra (normalized amplitude), (c) Variation of the spatial frequency as a function of the CHCF length.

Table 1
Insertion loss and the contrast of the different MZIs.

Design CHCF length (mm)	Insertion loss (dB)	Contrast (dB)	3 dB bandwidth (nm)
0.3	−13.30	9.38	9.92
0.4	−10.64	21.01	6.88
0.5	−6.52	31.18	5.22
0.6	−14.2	22.17	4.52
0.7	−13.32	16.05	3.92

write a linear relationship between the spatial frequency (ξ) and the length (L) [20],

$$\xi = \frac{1}{\lambda^2}\Delta n_{eff} L, \tag{2}$$

where the spatial frequency is the number of cycles per nm. It is vital to estimate the value of Δn_{eff} since using it, one can estimate the *FSR* of each MZI by knowing its length or vice versa. One way to find the ERID is by fabricating some MZIs using different lengths, as shown in Fig. 3 (a). The spatial frequencies were evaluated by applying the Fast Fourier Transform (FFT) to each spectrum, see Fig. 3 (b). It should be remembered that three sensors were fabricated for each CHCF length. Fig. 3 (c) shows the average of each spectral frequency related to each CHCF length and its associated error (standard deviation). It is possible to calculate the slope (ξ/L) with the help of the data of Fig. 3 (c), which is 0.195 ± 0.005 (nm^{-1}/mm). Using this slope, the central frequency of the spectrum (1575 nm), and the Eq. (2), we found that $\Delta n_{eff} = 0.484 \pm 0.005$. Knowing Δn_{eff} and using $L = \lambda^2/\Delta n_{eff} FSR$, where the value of *FSR* was measured directly from the OSA, we determined the physical length of the MZIs.

Table 2
Fabrication error of each length.

Design CHCF length (mm)	*FSR* (nm)*	Fabrication length error (mm)**	Fabrication error (%)***
0.3	17.06	0.004	1.397
0.4	13.16	0.011	2.646
0.5	9.94	0.012	2.369
0.6	8.45	0.014	2.280
0.7	7.41	0.008	1.178

*Average of the *FSR*. **Average absolute error of the fabrication process. ***Average percentage error relative to the sensor's length.

The fabrication error of this process can be evaluated by using the absolute error of each MZI, see Table 2. Column one shows the design lengths that want to be cut, column two exhibits the averages values of the *FSR*s of the devices. Finally, we can observe that the fabrication error is less than 3 % for all the CHCF lengths used in the experiment, which means that the process is highly repeatable.

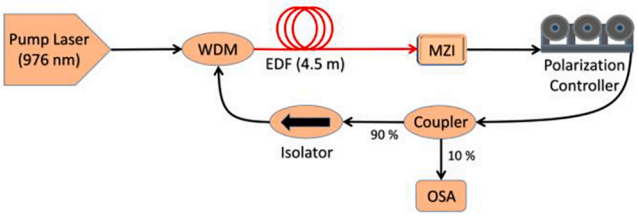

Fig. 4. Schematic of the fiber ring laser cavity developed using a MZI based on CHCF.

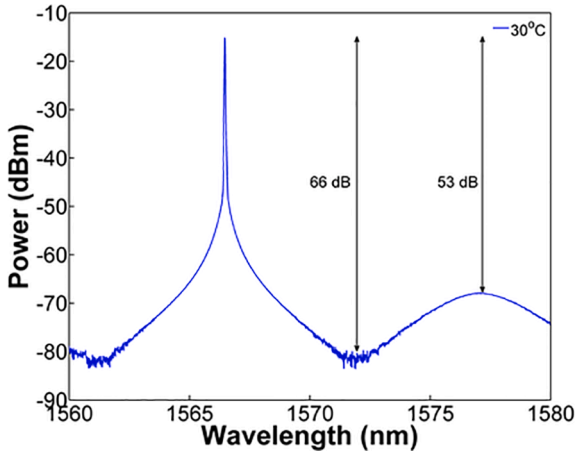

Fig. 5. Laser emission obtained from the ring fiber laser experimental setup.

3. Experimental setup

As mentioned in the last section, the filter with the design length of 0.5 mm (actual physical length of 0.48 mm, see Fig. 1 (b)) was used to implement a TEDFL, see Fig. 4. The ring fiber cavity laser consists of a pump laser diode (BL976-PAG700, Thorlabs) that launched light with a wavelength of 976 nm into the 4.5 m long EDF (Er80-8/125, Thorlabs), whose peak absorption at 1530 nm is 80 dB, through a 980/1550 wavelength division multiplexer (WDM) fiber coupler. A polarization controller (PC) was added in the cavity not only to obtain a higher SNR but also to get a more stable output power. An isolator was set in the laser cavity to protect the system against reflections and obtain unidirectional operation. An optical fiber coupler (90/10) was used to monitor the laser output by connecting the 10% port to the OSA, and the rest of the signal (90%) was sent back to the cavity for continuous laser generation. It is worth mentioning that the laser cavity length is approximately 25 m. Moreover, the laser was placed inside an acrylic box to avoid temperature fluctuations, and the MZI was kept at its operating temperature.

4. Results and discussion

It is important to highlight that the superposition of the transmission spectrum of the MZI and the gain spectrum of the EDF determine the laser emission wavelength. However, an initial adjustment of some parameters is required for optimum lasing operation. Therefore, using this MZI, we found a stable laser emission when the pump diode was set at a current of 400 mA. Additionally, the PC was adjusted to obtain a high SNR and stable output power, even though the MZI does not depend on polarization. After this initial adjustment in the PC and operating at a fixed temperature (30 °C), it was possible to obtain single laser emission centered at 1566.46 nm with a spectral width around 0.03 nm, and with a high SNR of 66 dB (also it has a SMSR of 53 dB), see Fig. 5. It should be mentioned that the minimum resolution of the OSA is 30 pm. These

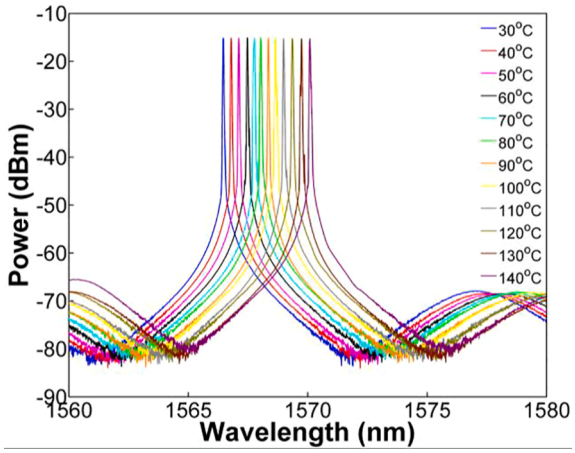

Fig. 6. Spectral response of the laser for temperatures from 30 to 140 °C.

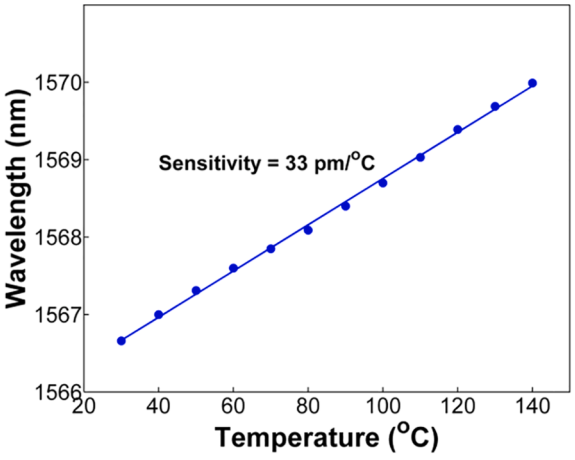

Fig. 7. Laser peak wavelength shift as a function of the applied temperature.

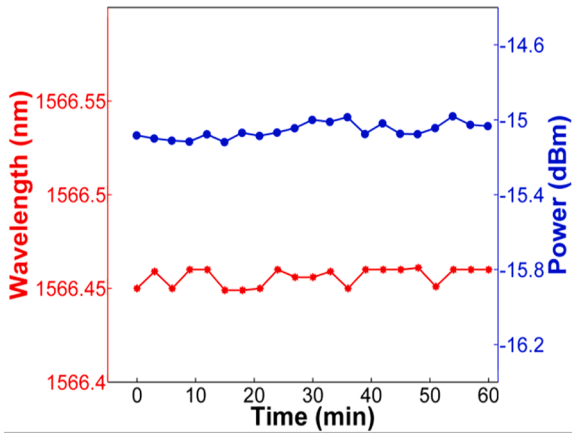

Fig. 8. Laser stability analysis.

results highlight the usefulness of the MZI as a filter inside a laser cavity since it generates a narrow linewidth with a high SNR. Remarkably, the improvements in the laser output are due to the MZI, whose total length is only 2.5 mm. The small size of the filter offers indisputable evidence that our fabrication technique is compelling, requires just a few fabrication steps, and is relatively simple compared with other systems [13,14,21–23].

Taking advantage of the temperature dependence of the MZI, as

Table 3
Laser parameters comparison with literature.

No.	Structure	Linewidth	Fluctuations	SNR/SMSR	Range/Sensitivity
1 [13]	MZI (aluminium coated)	<0.05nm	0.2 dB	55 dB/-	0 to 90 (90 °C) 28 pm/ °C
2 [19]	MZI (Tapered fiber)	–	–	50 dB/-	55 to 70 (15 °C) 1.09 nm/ °C
3 [20]	SMF-MMF-DCF-SMF	0.251 nm	–	44 dB/-	20 to 80 (60 °C) 18 pm/ °C
4 [21]	DPFI (fiber peanuts)	About 0.02 nm	0.03 nm 0.003 dB	-/50 dB	25 to 35 (10 °C) 1.24 nm/ °C
5	Our work (MMF-CHCF-MMF)	~ 0.03 nm	0.0108 nm 0.1379 dB	66/53 dB	30 to 140 (140 °C) 33 pm/ °C

mentioned in section 2, the filter was set on a hot plate (Thermo Scientific™, model HP88854100) for detuning laser emission as the temperature is increased. By changing the temperature from 30 to 140 °C, we can tune the laser emission from 1566.46 to 1570.09 nm, as shown in Fig. 6. It was found that the temperature sensitivity was 33 pm/°C, see Fig. 7. Moreover, we analyzed the stability of the single laser emission by monitoring the laser output every 3 min for one hour. It can be observed from Fig. 8 that the power and wavelength variations were 0.1379 dB and 0.0108 nm, respectively. These small variations of the laser emission (amplitude and wavelength) are due to the sensor's small temperature sensitivity, causing small temperature fluctuations (lower than 2 °C) that produce slight changes in the laser emission. As a result, a stable and tunable single laser emission was achieved.

In order to compare the performance of our laser to similar systems based on interferometer devices, we elaborated Table 3, which summarizes the structures and results from other research groups in the last years. The laser linewidth is similar in all the cases except structure three, which is slightly wider. The SNR and the SMSR of our laser are higher than the other lasers listed in Table 3. Regarding power and wavelength fluctuations, it can be said that the results of all lasers are similar, except for structure four, which demonstrates better performance. Finally, the sensitivities reported by structures two and four are higher than our laser. Nonetheless, the fabrication process of our filter is straightforward compared to the other filters since it does not need costly and complex methods like metal coating, tapering, or expensive specialty fibers.

5. Conclusion

In summary, a narrow linewidth and wavelength-tunable EDFL based on MZI was proposed and experimentally investigated. The MZI filter was fabricated by splicing a short length of CHCF between two small sections of MMFs. By inserting this filter into an EDFL, the laser emitted at 1566.46 nm, with a spectral width around 0.03 nm and an SNR of 66 dB. The TEDFL exhibited low power fluctuations (0.1379 dB) and practically no wavelength variations (0.0108 nm). The single-wavelength emission was also tuned from 1566.46 to 1570.09 nm by increasing the temperature of the filter. We should highlight that the fabrication process is cost-effective and highly reproducible, requiring minimal components for its operation.

CRediT authorship contribution statement

Sigifredo Marrujo-Garcia: Validation, Investigation, Visualization, Formal analysis, Writing – review & editing. **Luis A. Herrera-Piad:** Conceptualization, Validation, Investigation, Visualization, Formal analysis, Writing – original draft. **Iván Hernández-Romano:** Conceptualization, Methodology, Validation, Visualization, Formal analysis, Writing – original draft, Writing – review & editing, Supervision. **Daniel A. May-Arrioja:** Conceptualization, Methodology, Writing – review & editing, Supervision. **Vladimir P. Minkovich:** Resources, Writing – review & editing. **Miguel Torres-Cisneros:** Resources, Writing – review & editing.

Declaration of Competing Interest

The authors declare that they have no known competing financial interests or personal relationships that could have appeared to influence the work reported in this paper.

Acknowledgment

This work was supported in part by the Mexican National Council of Science and Technology (CONACyT) under Grant CB2017-2018-A1-S-31806, Grant CB2016-286368, and Grant CB2016-286629, in part by Universidad de Guanajuato under Grant CIIC-084/2021. S. Marrujo-García is grateful to CONACyT for the Ph. D scholarship. L. A. Herrera-Piad thanks to his postdoctoral scholarship from CONACyT (CB2016-286629).

References

[1] Z.-R. Lin, C.-K. Liu, G. Keiser, Tunable dual-wavelength erbium-doped fiber ring laser covering both C-band and L-band for high-speed communications, Optik 123 (1) (2012) 46–48.
[2] H.Y. Ryu, W.-K. Lee, H.S. Moon, H.S. Suh, Tunable erbium-doped fiber ring laser for applications of infrared absorption spectroscopy, Opt. Commun. 275 (2) (2007) 379–384.
[3] S.R. Chinn, E.A. Swanson, J.G. Fujimoto, Optical coherence tomography using a frequency-tunable optical source, Opt. Lett. 22 (5) (1997) 340–342.
[4] Z. Zhang, C. Mou, Z. Yan, K. Zhou, L. Zhang, S. Turitsyn, Sub-100 fs mode-locked erbium-doped fiber laser using a 45°-tilted fiber grating, Opt. Express 21 (23) (2013) 28192–28303.
[5] X. Feng, H.Y. Tam, P.K. Wai, Switchable multiwavelength erbium-doped fiber laser with a multimode fiber Bragg grating and photonic crystal fiber, IEEE Photonics Thecnol. Lett. 18 (9) (2006) 1088–1090.
[6] S.C. Feng, O. Xu, S.H. Lu, S.S. Jian, Switchable multi-wavelength erbium-doped fiber lasers based on a Mach-Zehnder interferometer using a twin-core fiber, Chin Phys. Lett. 24 (6) (2009) 1–4.
[7] H. Ahmad, A.A. Jasim, Stable C-band fiber laser with switchable multi-wavelength output using coupled microfiber Mach-Zehnder interferometer, Opt. Fiber Technol. 36 (6) (2017) 105–114.
[8] L. Zhang, Z. Tian, N. Chen, H. Han, C. Liu, K. Grattan, B. Rahman, Room-temperature power-stabilized narrow-linewidth tunable erbium-doped fiber ring laser based on cascaded mach-zehnder interferometers with different free spectral range for strain sensing, J. Lightw. Technol. 38 (7) (2020) 1966–1974.
[9] W. He, C. Shangguan, L. Zhu, M. Dong, F. Luo, Tunable and stable multi-wavelength erbium-doped fiber laser based on a double Sagnac comb filter with polarization maintaining fibers, Optik 137 (2017) 254–261.
[10] P. Wang, L. Wang, G. Shi, T. He, H. Li, Y. Liu, Stable multi-wavelength fiber laser with single-mode fiber in a Sagnac loop, Appl. Opt. 55 (12) (2016) 3339–3342.
[11] X. Liu, C. Lu, Self-stabilizing effect of four-wave mixing and its applications on multiwavelength erbium-doped fiber lasers, IEEE Photonics Lett. 17 (12) (2005) 2541–2543.
[12] X.M. Liu, Y. Chung, A. Lin, W. Zhao, K.Q. Lu, Y.S. Wang, T.Y. Zhang, Tunable and switchable multi-wavelength erbium-doped fiber laser with highly nonlinear photonic crystal fiber and polarization controllers, Laser Phys. Lett. 5 (12) (2008) 904–907.
[13] J.A. Martin-Vela, J.M. Sierra-Hernandez, E. Gallegos-Arellano, J.M. Estudillo-Ayala, M. Bianchetti, D. Jauregui-Vazquez, J.R. Reyes-Ayona, E.C. Silva-Alvarado, R. Rojas-Laguna, Switchable and tunable multi-wavelength fiber laser based on a coreoffset aluminum coated Mach-Zehnder interferometer, Optics Laser Technol. 125 (106039) (2020) 1–9.

[14] Q. Zhao, L. Pei, J. Zheng, M. Tang, Y. Xie, J. Li, T. Ning, Tunable and interval-adjustable multi-wavelength erbium-doped fiber laser based on cascaded filters with the assistance of NPR, Optics Laser Technol. 131 (106387) (2020) 1–8.
[15] Z. Tang, L. Liu, T. Benson, Z. Lian, S. Lou, Dual-wavelength interval tunable and multi-wavelength switchable high-performance fiber laser based on four-leaf clover suspended core fiber filter, Optics Laser Technol. 139 (106966) (2021) 1–8.
[16] S. Marrujo-García, S. Flores-Hernández, M. Torres-Cisneros, D. López-Cortés, D. Monzón-Hernández, D. A. May-Arrioja, and I. Hernández-Romano "Polymer Comparison on Temperature Sensors Based on Fiber-Optic Fabry-Perot Interferometer" In OSA Latin America Optics and Photonics Conference, Lima, Perú, 2018, pp. 1-2.
[17] L.A. Herrera-Piad, I. Hernández-Romano, D.A. May-Arrioja, V.P. Minkovich, M. Torres-Cisneros, Sensitivity enhancement of curvature fiber sensor based on polymer-coated capillary hollow-core fiber, Sensors 20 (3763) (2020) 1–13.
[18] J. Komma, C. Schwarz, G. Hofmann, D. Heinert, R. Nawrodt, Thermo-optic coefficient of silicon at 1550 nm and cryogenic temperatures, Appl. Phys. Lett. 101 (4) (2012), 041905.
[19] X. Li, S. Lin, J. Liang, Y. Zhang, H. Oigawa, T. Ueda, Fiber-optic temperature sensor based on difference of thermal expansion coefficient between fused silica and metallic materials, IEEE Photonics J. 4 (1) (2011) 155–162.
[20] H.Y. Choi, M. J. Kim, and B. H. Lee, "All-fiber Mach-Zehnder type interferometers formed in photonic crystal fiber" Opt. Express, vol. 15, no. 9, pp. 5711–5720, 2007.
[21] A. Martinez-Ríos, G. Anzueto-Sanchez, R. Selvas-Aguilar, A. Alberto Castillo Guzman, D. Toral-Acosta, V. Guzman-Ramos, V. M. Duran-Ramirez, J. A. Guerrero-Viramontes, and C. A. Calles-Arriaga "High Sensitivity Fiber Laser Temperature Sensor" IEEE Sensors J., vol. 15, no. 4, pp. 2399-2402, 2015.
[22] R.I. Álvarez-Tamayo, M. Duran-Sanchez, P. Prieto-Cortés, G. Salceda-Delgado, A. A. Castillo-Guzmán, R. Selvas-Aguilar, B. Ibarra-Escamilla, E.A. Kuzin, All-fiber laser curvature sensor using an in-fiber modal interferometer based on a double clad fiber and a multimode fiber structure, Sensors 17 (2744) (2017) 1–11.
[23] H. Wan, Y. Chen, Q. Zhou, Z. Shen, Z. Zhang, Tunable, single-wavelength fiber ring lasers based on rare earth-doped, double-peanut fiber interferometers, J. Lightw. Technol. 38 (6) (2020) 1501–1505.